Crystal structure, Hirshfeld surface analysis, and physicochemical studies of a new Cu(II) complex with 2-amino-4-methylpyrimidine

Kacem Klai, Sarra Soudani, Christian Jelsch, Frederic Lefebvre, Werner Kaminsky, Wataru Fujita, Cherif Ben Nasr, Kamel Kaabi

Published as https://doi.org/10.1016/j.molstruc.2019.05.027

Klai, K., Soudani, S., Jelsch, C., Lefebvre, F., Kaminsky, W., Fujita, W., ... & Kaabi, K.

(2019). *Journal of Molecular Structure*, *1194*, 297-304.

Crystal structure, Hirshfeld surface analysis, and physicochemical studies of a new Cu(II) complex with 2-amino-4-methylpyrimidine

Kacem Klai[a], Sarra Soudani[a], Christian Jelsch[b], Frédéric Lefebvre[c], Werner Kaminsky[d], Wataru Fujita[e], Cherif Ben Nasr[a], Kamel Kaabi[a*]

[a] Laboratoire de Chimie des Matériaux, Université de Carthage, Faculté des Sciences de Bizerte, 7021 Zarzouna, Tunisie.

[b] CRM^2, CNRS, Institut Jean Barriol, Université de Lorraine, Vandœuvre les Nancy Cedex, France.

[c] Laboratoire de Chimie Organométallique de Surface (LCOMS), Ecole Supérieure de Chimie Physique Electronique, 69626 Villeurbanne Cedex, France.

[d] Department of Chemistry, BOX 351700 University of Washington Seattle, WA 98195, USA.

[e] General Education, Faculty of Science and technology, Seikei University, Kichijoji-kita machi, Musashino 180-8633, Japan.

Abstract

The chemical preparation, crystal structure, magnetic study and spectroscopic characterization of the new Cu(II) complex with the monodentate ligand 2-amino-4-methylpyrimidine [$Cu_2(CH_3COO)_4(C_5N_3H_7)_2$] are reported. The copper atoms are surrounded by one nitrogen atom from one 2-amino-4-methylpyrimidine ligand and four oxygen atoms of CH_3COO^- groups yielding to a penta-coordination of the metal ion. In the structural arrangement, the amino group and the pyrimidine nitrogen atom of neighboring molecules are linked together through a pair of N-H…N hydrogen bonds forming a 1-D corrugated chain

running along the [111] direction wherein the complex molecules are located parallel to the (**a**, **c**) plane at z = ½. Intermolecular interactions were investigated by Hirshfeld surfaces and contact enrichment tools. Mulliken charge distribution, molecular electrostatic potential (MEP) maps and HOMO and LUMO energy gaps have been computed. The vibrational absorption bands were identified by infrared spectroscopy. Magnetic properties were also studied to characterize the complex.

Keywords: Copper(II) complex; X-ray structure; Hirshfeld surface; contact enrichment ratio; DFT calculations; magnetic properties.

1. Introduction

The design and construction of metal–organic coordination polymers are of current interest in the fields of supramolecular chemistry and crystal engineering. This interest stems from their huge variety of topologies and structural diversity and from their potential applications as functional materials, such as gas storage, ion-exchange, catalysis, magnetism, and molecular sensing [1-3]. The presence of more than one hetero atom in pyrimidine plays an important role in its coordination chemistry compared to that of pyridine bases [4-7]. Moreover, pyrimidine derived metal ion complexes have been extensively studied in recent years owing to their great variety of biological activity ranging from antimalarial, antibacterial, antitumoral, antiviral activities, etc. [8-17]. The chemistry of transition metal complexes with ligands of biological relevance in which the metal centers are in close proximity is one of the central themes of current research. This is especially true for copper complexes [18, 19], due to their versatile structural chemistry, their electrochemical and magnetic properties [20] and also because of their relevance as synthetic models [21, 22] for active sites of several metallo-enzymes [23]. The structural diversity of copper(II) complexes is largely related to the fact that a Cu(II) with d^9 configuration is Jahn-Teller active: a single unpaired d-electron occupies one of the d orbitals, which gives rise to structural flexibility and often highly distorted ligand coordination

geometries [3]. Polynuclear metal clusters have been widely used. Among them, poly-nuclear copper clusters are of especial interest due to their attracting structures as well as their potential applications in molecule-based magnets, multi-electron redox processes, and catalysis [2]. In this paper, we report the synthesis and the physicochemical characterization of a new Cu(II) dinuclear complex with the monodentate ligand 2-amino-4-methylpyrimidine which their binding characterized by low-energy delocalized π*-orbitals increases the possibility of modification in their optical, physico-chemical and electrochemical properties as well as the structural characteristics. The Hirshfeld surface analysis was conducted to fully characterize the intermolecular interactions and explain the crystalline architecture. Moreover, the complex was studied by spectroscopic study and DFT calculations were used for the interpretation of the vibration results. The magnetic susceptibility measurements are also presented.

2. Experimental

2. 1. Chemical preparation

A solution of $Cu(CH_3COO)_2$ (0.1 mmol) in water (5 mL) was added dropwise to a solution of 2-amino-4-methylpyrimidine (0.1 mmol) in water (10 mL). After stirring for 30 min, the mixture was filtered. Crystals suitable for X-ray analysis were obtained after a week by evaporating the filtrate at room temperature (yield = 76%).

2.2. Investigation techniques

The characterization of the investigated compounds was performed using X-ray diffraction, magnetic measurements and IR spectroscopy.

2. 2. 1. X-ray single crystal structural analysis

A purple prism, measuring 0.27 x 0.20 x 0.10 mm^3 was mounted on a loop with oil. Data were collected at -173^oC on a Bruker APEX II single crystal X-ray diffractometer, Mo-radiation. All non-hydrogen atoms were refined anisotropically by full-matrix least-squares.

The drawings were made with Diamond [24] Crystal data and experimental parameters used for the intensity data collection are summarized in Table 1.

2. 2. 2. Magnetic measurements

Magnetic measurements were carried out on microcrystalline samples with a SQUID magnetometer (Quantum Design XL-7). The *dc* magnetic measurements were carried out under 500 Oe in the 2–300 K temperature range. The raw data were corrected for diamagnetism estimated by the Pascal rule, and the molar paramagnetic susceptibilities were calculated.

2. 2.3. IR measurements

The IR spectra were recorded in the range 4000–400 cm^{-1} with a ‘‘Perkin–Elmer FTIR’’ spectrophotometer 1000 using samples dispersed in spectroscopically pure KBr and pressed into a pellet.

3. Results and discussion

3.1. X-ray diffraction study

X-ray crystal structure analysis reveals that the complex crystallizes in the triclinic space group $P\bar{1}$ (Table 1). Each molecule in the unit cell is a dimer having four bidentate CH_3COO^- groups binding two copper ions in a bridging bidentate fashion, resulting in a paddlewheel structure (Fig. 1). The Cu–Cu distance within the dinuclear unit is 2.6479 (3) Å which is comparable to similar bonds found in other coordination compounds [25, 26]. The copper atoms are coordinated by one nitrogen atom from one 2-amino-4-methylpyrimidine ligand and four oxygen atoms of CH_3COO^- groups to yield a penta-coordination for the metal ion.

The degree of distortion from a regular trigonal bipyramid can be quantified by the structural index τ, namely the Addison parameter $\tau = (\beta - \alpha)/60$ with β and α being the two largest angles [27] (where $\tau = 0$ and 1 for the perfect square pyramidal and trigonal bipyramidal geometries, respectively). The calculated τ value of the title compound is τ(Cu) = 0.0003 (β and α values are 167.64(4)° and 167.62(4) °, respectively), indicating a quite small distortion from

the regular square pyramid. This value is observed in other similar compounds [28]. The cis angles around the Cu atom which range from 88.47 (5)° to 90.71 (5)° also show that the CuO_4N species has a slightly distorted square pyramidal geometry (Fig. 1, Table 2). Basal Cu–O bond distances (Table 2) vary in the range 1.9625 (11) – 1.9747 (15) Å and are somewhat shorter than the apical Cu–N1 bond distance (Cu– N1 = 2.2224 (11) Å). This fact may be ascribed to a Jahn-Teller distortion. These bond distances around the Cu atom are comparable to similar bonds found in other coordination compounds [25, 29].

In the structural arrangement, the amino group and the pyrimidine nitrogen of neighboring molecules are linked together through a pair of N-H…N hydrogen bonds (Table 3) forming a cyclic hydrogen bonded motif with graph set notation, $R_2^2(8)$ (Fig. 2). These hydrogen bonds stabilize the dimeric structure and stack at top one another to form a 1-D corrugated chain running along the [111] direction (Fig. 2 and Fig. S1) wherein the complex molecules are located parallel to the (**a**, **c**) plane at $y = ½$ (Fig. S1).

The intramolecular hydrogen bond N3—H···O3 (Table 3) does also contribute to the robustness of the structure of this compound. Within the organic ligand 4-amino-6-methylpyrimidine, an examination of the C-N bond distance of the NH_2 group shows that C5-N3 [1.330 (2) Å] is short for a C-N single bond, but still not quite as contracted as one would expect for a fully established C=N double bond. This bond length feature is consistent with an imino resonance form as it is commonly found for C-N single bond involving sp^2 hybridized C and N atoms [30, 31].

3.2. Hirshfeld surface analysis

Analysis of intermolecular interactions using the Hirshfeld surface represents a major tool in enabling supramolecular chemists and crystal engineers to gain insight into understanding the crystal packing. These surfaces are constructed based on the electron distribution calculated as the sum of spherical atom electron densities. In order to visualize and

explore all intermolecular contacts in the molecular structure, the MoProViewer software [32] was used to carry out Hirshfeld surface analysis and compute contact types and their enrichment. The enrichment ratio E_{XY} for a pair of elements (X,Y) is defined as the ratio between the proportion of actual contacts in the crystal (C_{XY}) and the theoretical proportion of equidistributed random contacts R_{XY}.

$$E_{XY} = C_{XY} / R_{XY} \qquad (1)$$

An enrichment ratio larger than unity reveals that a pair of elements has a high propensity to form contacts in the crystal, while pairs which tend to avoid contacts with each other should yield an E value lower than unity.

A large range of properties can be visualized on the Hirshfeld surface with Crystal Explorer [33] including the distance of atoms external, de, and internal, di, to the surface. The intermolecular distance information on the surface can be condensed into a two-dimensional histogram of de and di, which is a unique fingerprint for molecules in a crystal structure. The fingerprint plots of the main interactions are shown in Fig. 3. The spikes at short distances are due to the H…O hydrogen bonds and Cu…O ionic bridges.

The nature of the intermolecular contacts in the crystal structure is shown in Table 4. The enrichment ratios [34, 35] of contacts between the different chemical species were computed in order to highlight which interactions are over-represented with respect to equiprobable contacts computed from the surface composition. The Hirshfeld surfaces are shown in Fig. 4.

Globally, hydrogen occupies the largest proportion of the Hirshfeld surface, reaching 44.7%, most of which is constituted by the hydrophobic Hc type. Consequently, the hydrophobic contacts Hc…Hc and Hc…C represent, with the Cu…O ionic bridges, the most represented contacts in the crystal packing. The occurrence of these hydrophobic contacts is

slightly enriched at *E* = 1.1 and 1.4, respectively. The hydrophobic C…C contact are rare but more enriched at *E*=1.8 due to π…π stacking between aromatic pyrimidine cycles. Globally, hydrophobic contacts involving C and Hc atoms of the organic molecule and the acetate anions represent as much as 40% of the contact surface.

The complexation of the Cu(II) cation by two carboxylate groups results in the strongest enrichment *E*(O,Cu)=3.5 while the copper…nitrogen interaction is also over-represented. The Hn hydrogen atoms have a significant partial charge and have the ability to form strong hydrogen bonds with the nitrogen and oxygen atoms. There are only one N-H…O and one N-H…N strong H-bonds in the crystal structure (Table 3). The Hn…N contacts are indeed quite enriched (*E* = 2.6), while Hn…O hydrogen bonds do also occur but are less favored, due to competition with $Cu^{++}…O^{\delta-}$ which constitutes the strongest electrostatic interaction in the title compound crystal. All the self-contacts between charged atom types (Cu++, Hn, O, N) are unfavorable from an electrostatic point of view and are avoided with enrichment ratios close to zero or lower than 0.5.

3.3. DFT calculations

DFT calculations were undertaken on the new Cu(II) complex $[Cu_2(CH_3COO)_4(C_5N_3H_7)_2]$ with the Gaussian 09 program [36]. The calculations were made on one isolated complex in gaseous phase. The coordinates of all atoms except protons were taken from the X-ray structure while those of hydrogen atoms were optimized by using the B3LYP/6-31+G* method. Both the singlet and triplet states were studied. The triplet state was found to be more stable by ca. 30 $kcal.mol^{-1}$ than the singlet one and so only this state was studied in the following.

HOMO-LUMO analysis.

The frontier molecular orbitals determine the way a molecule interacts with other entities and helps to determine its kinetic stability and chemical reactivity of molecules. The HOMO-LUMO orbitals are displayed in **Fig. 5.**

The highest occupied molecular orbital (HOMO) is located mainly on the two organic molecules (calculated energy of -6.271 eV) while the lowest unoccupied molecular is also localized on both molecules but on different atoms than the HOMO orbital (calculated energy of LUMO is -1.123 eV). The large energy gap between the HOMO and LUMO orbitals in the title compound is 5.148 eV and characterizes a high kinetic stability and a high chemical hardness [37, 38]. Indeed, it is energetically unfavorable to add electron to a high-lying LUMO or to extract electrons from a low-lying HOMO [39]. The energy distribution of the different orbitals is given in **Fig. 6.**

Molecular Electrostatic Potential Analysis

The molecular electrostatic potential of $[Cu_2(CH_3COO)_4(C_5N_3H_7)_2]$ has also been computed and is shown in **Fig. 7**. As it can be seen from this figure, the electrostatic potential maps are color-coded and are subdivided into many regions where those various colors are used to identify different potentials. Blue and red colors indicate the positive and negative potentials, respectively. Intermediate potentials are assigned to colors according to the following color spectrum: red < orange < yellow< green < blue. The MEP surface calculated for the title compound shows that the potential energy is positive over the organic cation and around the nitrogen atoms while the negative MEP described by red region around the oxygen atoms of the acetate groups. According to these results, we can say that there is a global electrostatic attraction between the 2-amino-4-methylpyrimidine ligands and the oxygen atoms of CH_3COO^- groups to yield a penta-coordination for the metal ion.

Mulliken population analysis

The Mulliken charge distribution [40, 41] of all atoms in the title compound is given in Table 5. All atoms in the asymmetric unit are listed and for the acetate groups two values are given as there are two different molecules. The atoms of the organic molecule are numbered as follows:

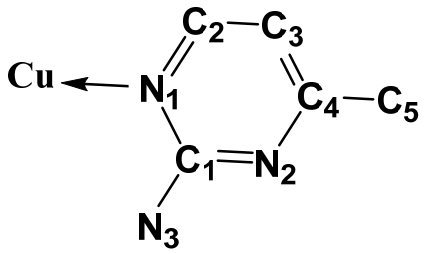

The atomic charge distribution shows that the oxygen atoms have negative charges of (-0.274461 & -0.428773) and (-0.231182 &-0.293471) respectively and that the copper ion has also a negative charge (-0.217248). When summing the charges on the atoms of the acetate groups values of -0.12 and -0.20 are obtained, showing that an electronic transfer occurred between the acetate groups and copper. In contrast the charge on the organic molecule is positive, due to a transfer of electrons from nitrogen to copper.

3.4. Magnetic susceptibility measurements

Fig. 8 shows the temperature dependence of the paramagnetic susceptibility χ_P per 1 mol of Cu in (this compound). The χ_P value decreased with a decrease in temperature down to approximately 50 K. This observation suggests that an antiferromagnetic interaction between the copper ions works in the dimer and that (this compound) has a diamagnetic ground state. The χ_P value increased with a further decrease in temperature. This is due to contribution of impurities or lattice defects. The magnetic behavior is very similar to that of $Cu(CH_3CO_2)_2.H_2O$ [42]. Based on the structure, we interpreted the magnetic data using the following equation,

$$\chi_p = \frac{Ng^2\mu_B^2}{k_B T}\frac{1}{3+\exp\left(\frac{-2J}{k_B T}\right)} + N\alpha + \frac{C_{imp}}{T} \quad (1)$$

wherer N is the Avogadro constant, g is g-factor, μ_B is the Bohr magneton, k_B is the Boltzmann constant, J is the intra-dimer magnetic coupling constant, $N\alpha$ is contribution of temperature-independent paramagnetism, and C_{imp} is the Curie constant. In eq. (1), the first term is the Bleaney-Bowers model [43] for 1 mole of copper atoms and expresses the paramagnetic contribution of the copper dimers. The third term corresponds to contribution of impurities and so on in the low temperature region, assuming the Curie behavior [44]. The solid curve in Fig.9 is the theoretical best-fit with the parameters; g = 2.11, $2J/k_B$= –496 K, 55 x 10^{-6} emu mol^{-1}, and 0.0010 emu K mol^{-1}. These value are consistent with those of $Cu(CH_3CO_2)_2.H_2O$ [42].

3.5. IR spectroscopy

The IR spectrum of the dimeric Cu(II) complex is shown in **Fig. 9**. The asymmetric and symmetric COO stretching vibrations of carboxylate give bands at 1558 and 1405 cm^{-1}, respectively. These bands are characteristic of dicopper tetracarboxylate complexes [45]. The attachment of carboxylate to Cu(II) ion through oxygen was further supported by the appearance of the absorption band at 415 cm^{-1}, corresponding to Cu–O. The value of $\Delta\nu$ ={ν_{asym}(OCO)- ν_{sym}(OCO)} calculated for the complex was 178 cm^{-1}, indicating a bridging bidentate coordination for carboxylate in the complex [46, 47]. The C=N stretching bands were observed at 1625 cm^{-1}. The large band spreading between 3600 and 2400 cm^{-1} corresponds to the asymmetric and symmetric stretching vibrations of the methyl and N-H groups.

DFT calculations of the infrared spectrum was made on the geometry obtained after optimization of the protons. The resulting IR spectrum between 4000 and 500 cm^{-1}, shown on **Fig. 10**, is very similar to the experimental one. A close agreement between the experimental and theoretical wave numbers is mostly achieved in the finger print region as shown in **Fig. 11**. Thus, the precision is well-sufficient to assign the experimental frequencies and to confirm the attributions proposed above.

4. Conclusion

In summary, a novel organic–inorganic hybrid compound, $[Cu_2(CH_3COO)_4(C_5N_3H_7)_2]$, has been synthesized at room temperature by slow evaporation. This compound belongs to the triclinic system with the space group P-1. The crystal packing is driven by the complexation of Cu(II) cation by two carboxylates groups and two nitrogen atoms; the remaining favorable interactions are mainly a N-H…O and N-H…N hydrogen and hydrophobic contacts between Hc and C atoms. As for the calculated DFT, it allowed to complete the experimental results and to propose a rigorous assignment for the observed IR bands of the title compound. In fact, the vibrational spectrum calculated by DFT/B3LYP/LanL2DZ method is in good agreement with the experimental results. Moreover, the HOMO-LUMO energy gap suggests a good stability of this compound.

Acknowledgment

The authors are grateful to the Tunisian Ministry of Higher Education and Scientific Research for financial support.

Supplementary data

Crystallographic data for the structural analysis have been deposited at the Cambridge Crystallographic Data Centre, CCDC No 1828793. These data can be obtained free of charge via http://www.ccdc.cam.ac.uk/conts/retrieving.html, or from the CCDC, 12 Union Road, Cambridge, CB2 1EZ, UK: fax: (+44) 01223-336-033; e-mail: deposit@ccdc.cam.ac.

References

[1] (a) K. Sumida, D.L. Rogow, J.A. Mason, T.M. McDonald, E.D. Bloch, Z.R. Herm, T.H. Bae, J.R. Long, Chem. Rev. **112**, 724 (2012).

(b) R.B. Getman, Y.-S. Bae, C.E. Wilmer, R.Q. Snurr, Chem. Rev. **112**, 703 (2012).

[2] (a) P. Dechambenoit, J.R. Long, Chem. Soc. Rev. **40**, 3249 (2011).

(b) E. Coronado, G.M. Espallargas, Chem. Soc. Rev. **42**, 1525 (2013).

(c) W.-X. Zhang, P.-Q. Liao, R.-B. Lin, Y.-S. Wei, M.-H. Zeng, X.-M. Chen, Coordin. Chem. Rev. **293-294**, 278 (2015).

[3] (a) L.E. Kreno, K. Leong, O.K. Farha, M. Allendorf, R.P. Van Duyne, J.T. Hupp, Chem. Rev. **112**, 1105 (2012).

(b) Y. Cui, Y. Yue, G. Qian, B. Chen, Chem. Rev. **112**, 1126 (2012).

(c) Z. Hu, B.J. Deibert, J. Li, Chem. Soc. Rev. **43**, 5815 (2014).

[4] F. Zamora, M. Kunsman, M. Sabat, B. Lippart, Inorg. Chem. **36**, 1583 (1997).

[5] M. Louloudi, Y. Deligiannakis, J.P. Tuchagues, B. Donnadien, N. Nadjiliadis, Inorg. Chem. **36**, 6335 (1997).

[6] F. Jolibois, J. Cadet, A. Grand, R. Subra, N. Raga, V. Barone, J. Am. Chem. Soc. **120**, 1864 (1998).

[7] A. R. Katritzky, C.W. Pees, A.J. Boulton, C. Mckillop, J. Heterocycl, Chem. **3**, 57 (1984).

[8] E.S. Roper, Coord. Chem. Rev. **61**, 115 (1985).

[9] J.S. Casas, E.E. Castellans, M.D. Louce, J. Ellena, A. Sanchez, J. Sordo, C. Taboada, J. Inorg. Biochem. **11**, 1858 (2006).

[10] M.J. Campbell, Coord. Chem. Rev. **15**, 297 (1975).

[11] D.X. West, S.B. Padhye, P.B. Sonawane, Struct. Bond (Berlin) **76**, 1 (1991).

[12] Y.P. Tian, C.Y. Duan, Z.L. Lu, X.Z. You, H.K. Fun, S. Kandasamy, Polyhedron **15**, 2263 (1996).

[13] S.K. Jain, B.S. Garg, Y.K. Boon, J.P. Scovill, D.L. Klayman, Spectrochim. Acta **24**, 407 (1985).

[14] S.B. Padhye, G.B. Kanffman, Coord. Chem. Rev. **63**, 127 (1985).

[15] D.X. West, A.E. Liberta, S.B. Padhye, R.C. Chilate, P.B. Sonawane, A.S. Kumbhar, R.G. Yerande, Coord. Chem. Rev. **123**, 49 (1993).

[16] T.S. Lobana, P.K. Bhatia, J. Sci. Ind. Res. **48**, 394 (1989).

[17] M.C. Rodriguez-Arguelles, S.J. Pinelli, J. Inorg. Biochem. **58**, 157 (1995).

[18] K. D. Karlin, S. Kaderli, A. D. Zuberber, Acc. Chem. Res., **30**, 139 (1997).

[19] P. A. Vigato, S. Tamburini, D. E. Fenton, Coord. Chem. Rev. **106**, 25 (1990).

[20] R.Guptam S.Mukherjee, R.Mukherjee; J.Chem. Dalton Trans., 4025 (1999).

[21] C.A. Reed, R.D. Orosz; Spin Coupling Concepts in Bioinorganic Chemistry, in: C.J.OConor, (Ed); World Scientific, Singapore, **351** (1993).

[22] E.I. Solomon, U.M. Sundaram, T.E. Machonkin, Chem. Rev., **96**, 2563 (1996).

[23] F. Zippel, F. Ahlers, R. Werner, W. Haaze, H.F. Noltine, B. Krebs, Inorg.Chem., **35**, 3409 (1996).

[24] Bruker, APEX2 (Version 2.1-4), SAINT (Version 7.34A), SADABS (Version 2007/4), Bruker AXS Inc, Madison, Wisconsin, USA, (2007).

[35] Y. B. Dong, J. P. Ma, M. D. Smith, R. Q. Huang, B. Tang, D. Chen, & H. C. zur Loye, . Solid state sciences, **4**, 1313 (2002).

[26] M. Iqbal, S. Ali, Z. U. Rehman, N. Muhammad, M.Sohail, V. Pandarinathan, J. Coord. Chem. **67**, 1731 (2014).

[27] A. W. Addison, N. T. Rao, J. Reedijk, J. van Rijn, G. C.Verschoor, J. Chem. Soc., Dalton Trans 1349 (1984).

[28] C. Hopa, I. Cokay, Acta Crystallogr., Sect. C: Cryst. Struct. Commun **72**, 149 (2016).

[29] H. -K. Liu, W.-Y. Sun, W. -X. Tong, T. Yamamoto, N. Ueyama, Inorg. Chem. **38**, 6313 (1999).

[30] K. Kaabi, M. El Glaoui, V. Ferretti, M. Zeller, C. Ben Nasr, Acta Cryst. E, **67**, 2507 (2011).

[31] M. B. Nasr, F. Lefebvre, C. B. Nasr, Am. J. Anal. Chem. **6**, 446 (2015).

[32] B. Guillot, E. Enrique, L. Huder, C. Jelsch, MoProViewer, Acta Cryst., A**70**, 279 (2014).

[33] M. A. Spackman, J. J. McKinnon, Finger printing inter molecular interactions in Molecular crystals, Cryst. Eng. Comm., **4**, 378 (2002).

[34] C. Jelsch, K. Ejsmont, L. Huder, IUCrJ., **1**, 119 (2014).

[35] C. Jelsch, S. Soudani, C. Ben Nasr, IUCrJ, **2**, 327 (2015).

[36] M. J. Frisch, G.W. Trucks, H.B. Schlegel, G.E. Scuseria, M.A. Robb, J.R. Cheeseman, G. Scalmani, V. Barone, B. Mennucci, G. A. Petersson, H. Nakatsuji, M. Caricato, X. Li, H.P. Hratchian, A. F. Izmaylov, J. Bloino, G. Zheng, J. L. Sonnenberg, M. Hada, M. Ehara, K. Toyota, R. Fukuda, J. Hasegawa, M. Ishida, T. Nakajima, Y. Honda, O. Kitao, H. Nakai, T. Vreven, J. A. Montgomery Jr., J.E. Peralta, F. Ogliaro, M. Bearpark, J. J. Heyd, E. Brothers, K. N. Kudin, V. N. Staroverov, T. Keith, R. Kobayashi, J. Normand, K. Raghavachari, A. Rendell, J. C. Burant, S. S. Iyengar, J. Tomasi, M. Cossi, N. Rega, J. M. Millam, M. Klene, J. E. Knox, J. B. Cross, V. Bakken, C. Adamo, J. Jaramillo, R.

Gomperts, R. E. Stratmann, O. Yazyev, A. J. Austin, R. Cammi, C. Pomelli, J.W. Ochterski, R. L. Martin, K. Morokuma, V. G. Zakrzewski, G. A. Voth, P. Salvador, J. J. Dannenberg, S. Dapprich, A. D. Daniels, O. Farkas, J. B. Foresman, J.V. Ortiz, J. Cioslowski, D. J. Fox, Gaussian 09,Revision B.01 Gaussian, Inc., Wallingford CT, (2010).

[37] R. G. Parr, R.G. Pearson, , J. Am. Chem. Soc. **105**, 7512 (1983).

[38] R. G. Pearson, Proc. Natl. Acad. Sci. USA **83**, 8440 (1986).

[39] H. Saeidian, M. Sahandi, J. Mol. Struct. **1100** 486 (2015).

[40] D. Arul Dhas, I. Hubert Joe, S.D.D. Roy, T.H. Freeda, Acta A **177**, 36 (2010).

[41] R.S. Mulliken, J. Chem. Phys. **23**, 1833 (1955).

[42] B.N. Figgis and R. L.Martin, J. Chern. Soc. 3837 (1956).

[43] B. Bleaney and K. D. Bowers Proc. Roy. Soc. (London) Ser. A **214**, 451 (1952).

[44] R. L. Carlin, Magnetochemistry, Springer, (1989).

[45] A.Doyle, J. Felcman, M. Teresa, M.L. Braganc, Polyhedron, **19**, 2621 (2000).

[46] G. Eng, X. Song, A. Zapata, A.C. de Dios, L. Casabiana, R.D. Pike. J. Organomet. Chem. **692**, 1398 (2007).

[47] G.B. Deacon, R.J. Phillips. Coord. Chem. Rev. **33**, 227 (1980).

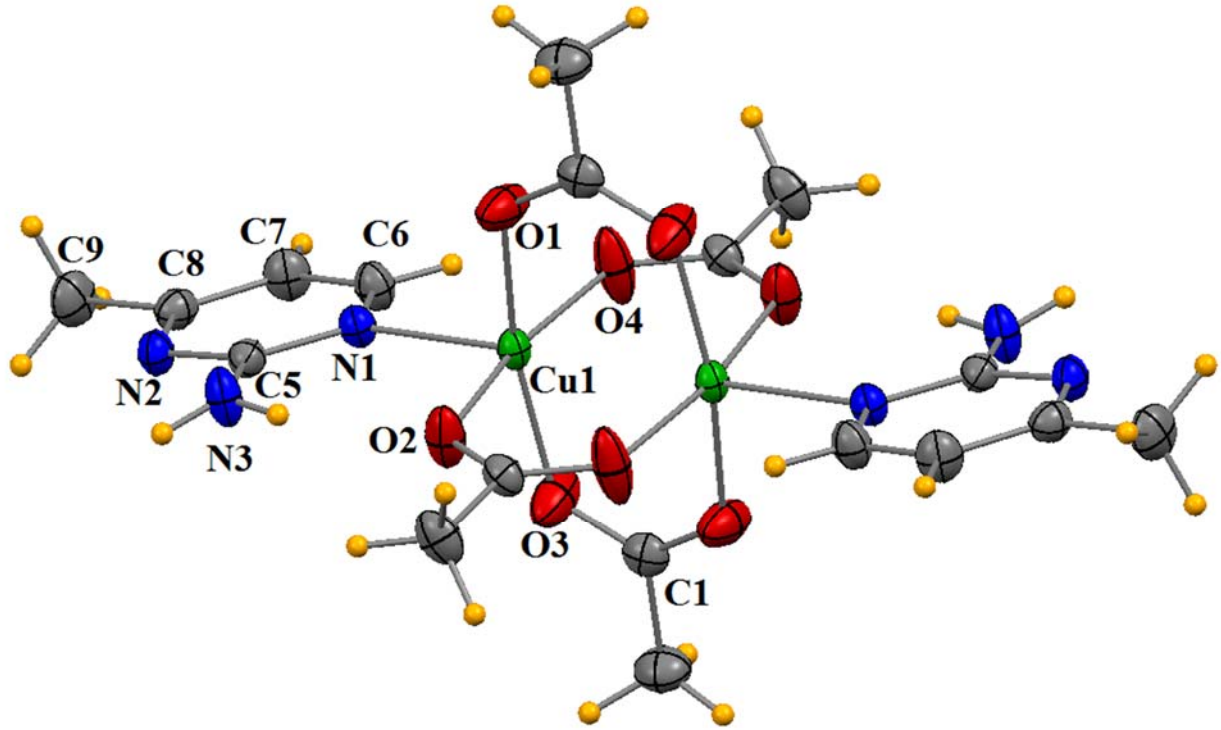

Fig. 1 ORTEP of the title compound with displacement ellipsoids drawn at the 40% probability

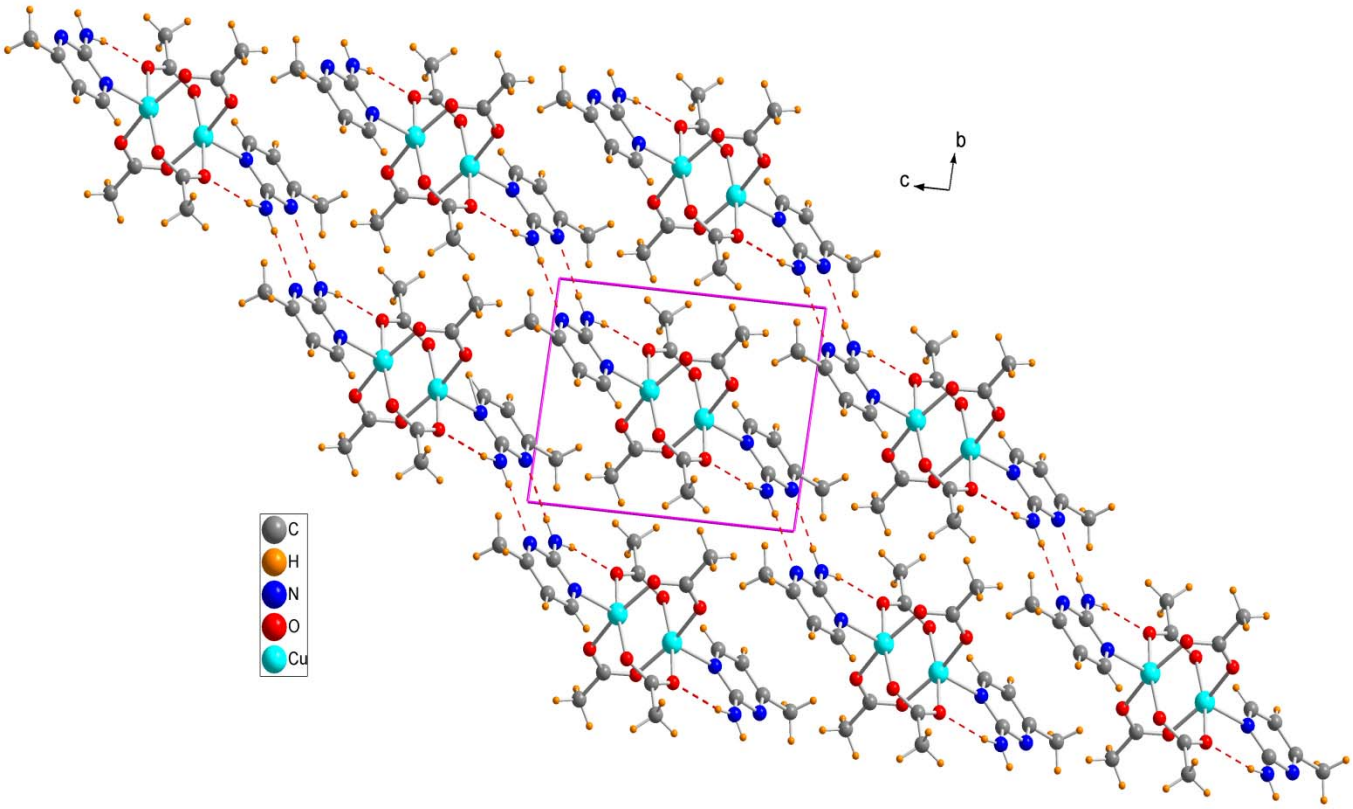

Fig. 2 Crystal packing arrangement of $[Cu_2(CH_3COO)_4(C_5N_3H_7)_2]$ viewed along *a*-axis. Dotted lines indicate hydrogen bonds.

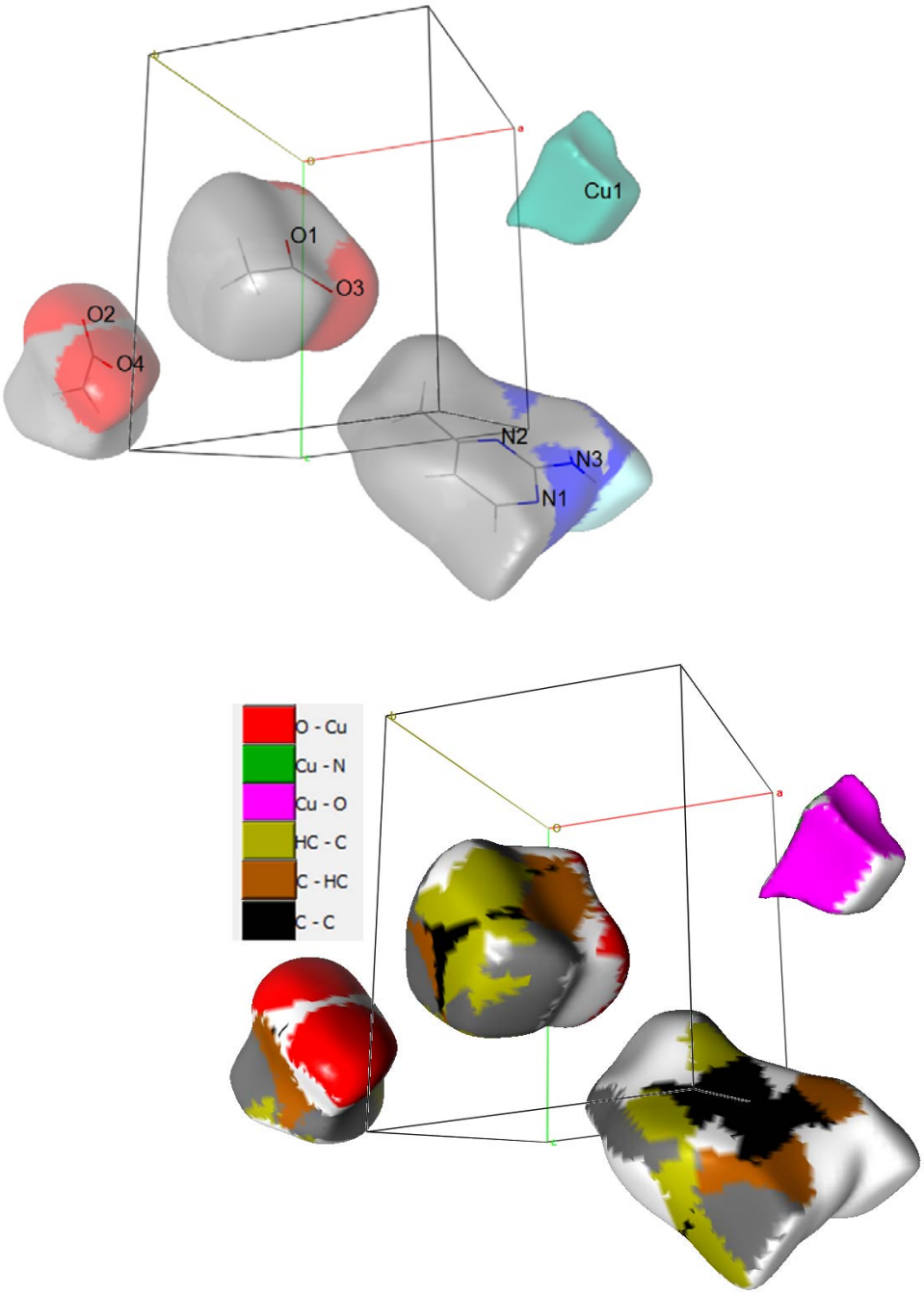

Fig. 3 Hirshfeld surface around the organic moiety, the Cu(II) cation and the two acetate anions. In order to have integral surfaces, moieties not in contact with each other were selected in the crystal packing. (a) The colors are according to the interior atom contributing most to the electron density. Oxygen: red, nitrogen: blue, hydrogen Hc: grey, Hydrogen Hn: light blue, carbon: grey, copper: green. (b) coloring according to the major contact types.

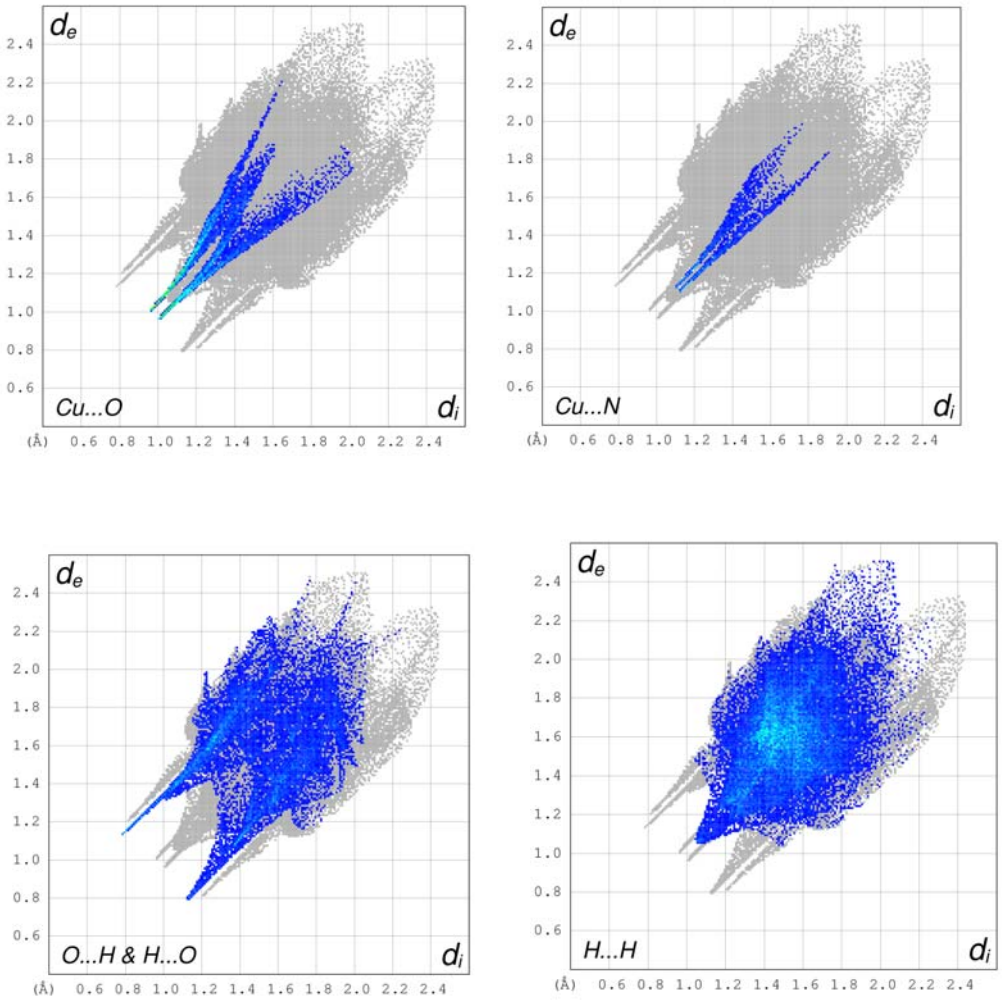

Fig. 4 2D Fingerprint plot of the main interactions (reciprocal interactions are merged).

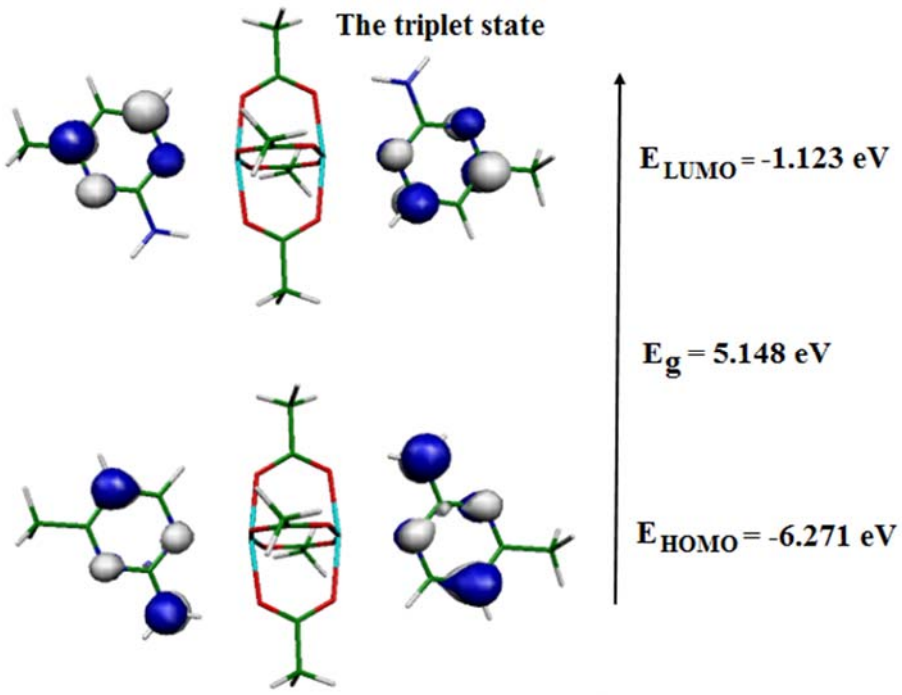

Fig. 5 HOMO-LUMO orbitals of $[Cu_2(CH_3COO)_4(C_5N_3H_7)_2]$.

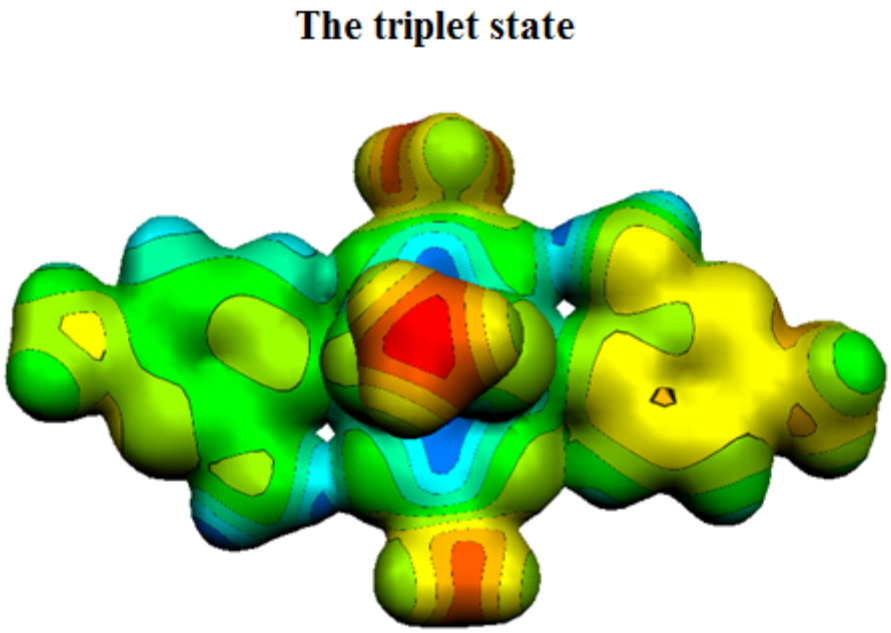

Fig. 6 Molecular Electrostatic Potential maps of the title compound.

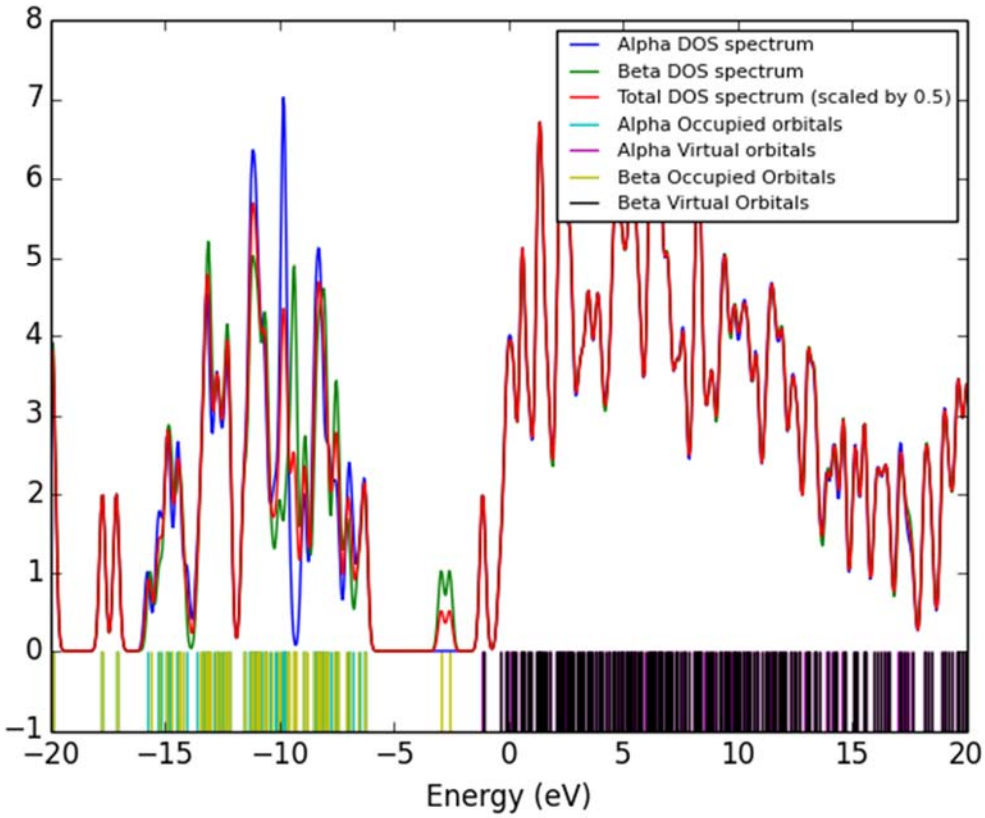

Fig. 7 The energy distribution of the different orbitals for the title compound.

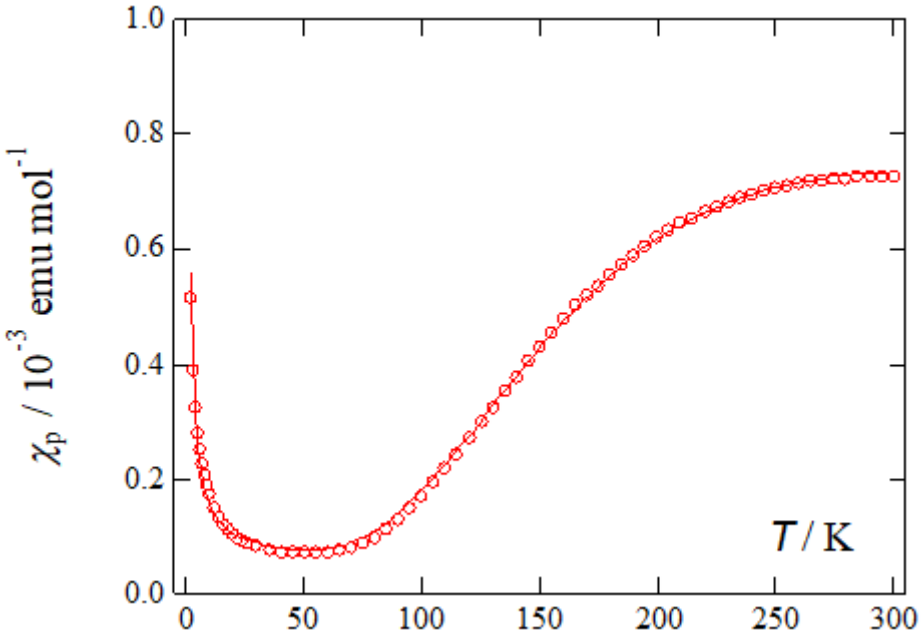

Fig. 8 Temperature dependence of the paramagnetic susceptibility, χ_p, of $[Cu_2(CH_3COO)_4(C_5N_3H_7)_2]$. The solid line shows the theoretical best-fit of the equation including the three terms of the Bleaney-Bowers model, diamagnetic susceptibility and Curie impurities.

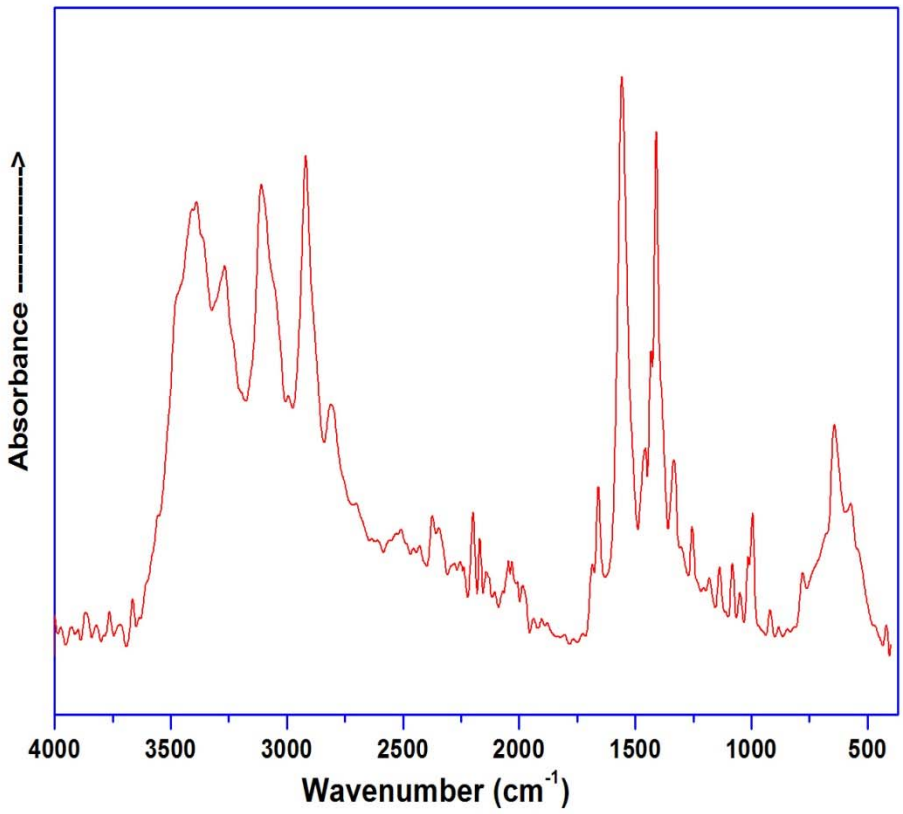

Fig. 9 Infrared absorption spectrum of $[Cu_2(CH_3COO)_4(C_5N_3H_7)_2]$

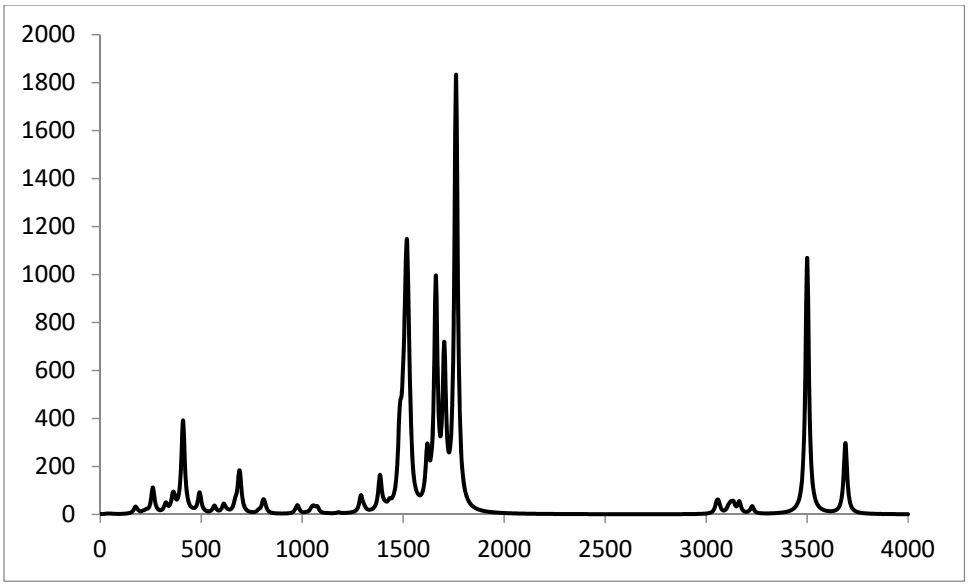

Fig. 10 Calculated IR absorption spectrum of the title compound.

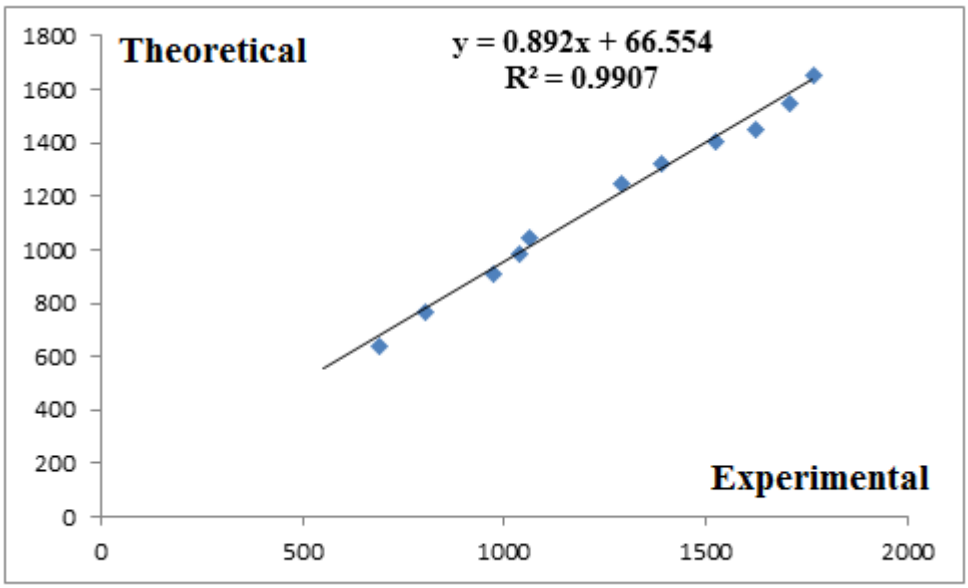

Fig. 11 Comparison between experimental and calculated IR frequencies.

Table 1. Experimental details of $[Cu_2(CH_3COO)_4(C_5N_3H_7)_2]$.

Crystal data	
Chemical formula	$C_{18}H_{26}Cu_2N_6O_8$
M_r	581.53
Crystal system, space group	Triclinic, P-1
Temperature (K)	100
a, b, c (Å)	7.3184 (3), 8.3106 (3), 10.2559 (4)
α, β, γ (°)	90.243 (2), 97.481 (2), 113.329 (2)
V (Å^3)	566.83 (4)
Z	1
Radiation type	Mo $K\alpha$
μ (mm^{-1})	1.93
Crystal size (mm)	0.27 × 0.2 × 0.1
Data collection	
Diffractometer	Bruker APEX II
Absorption correction:	multi-scan
No. of measured, independent and observed [$I > 2\sigma(I)$] reflections	20708, 2848, 2722
R_{int}	0.020
$(\sin \theta/\lambda)_{max}$ (Å^{-1})	0.670
Refinement	
$R[F^2 > 2\sigma(F^2)]$, $wR(F^2)$, S	0.020, 0.054, 1.10
No. of reflections	2848
No. of parameters	163
$\Delta\rho_{max}$, $\Delta\rho_{min}$ (e Å^{-3})	0.40, −0.36

Table 2. Selected bond distances and angles (Å, º) in the title complex.

Symmetry code: (i) −*x*+1, −*y*+1, −*z*+1

N1—Cu1	2.2224 (11)	O2—Cu1—O1	90.71 (5)
O1—Cu1	1.9726 (10)	O4—Cu1—O3	88.47 (5)
O2—Cu1	1.9639 (11)	O2—Cu1—O3	88.58 (5)
O3—Cu1	1.9747 (10)	O1—Cu1—O3	167.62 (4)
O4—Cu1	1.9625 (11)	O4—Cu1— N1	99.29 (4)
Cu1—Cu1 ^{i}	2.6479 (3)	O2—Cu1— N1	93.06 (4)
O4—Cu1—O2	167.64 (4)	O1—Cu1— N1	92.48 (4)
O4—Cu1—O1	89.61 (5)	O3—Cu1— N1	99.88 (4)

Table 3. Hydrogen-bond geometry (Å, °) in the title complex in the title complex

D—H···*A*	*D*—H	H···*A*	*D*···*A*	*D*—H···*A*
N3—H3O···N2^{ii}	0.84 (1)	2.18 (1)	3.0233 (16)	177 (2)
N3—H3P···O3	0.85 (1)	2.07 (1)	2.8682 (15)	158 (1)

Symmetry code: (ii) −*x*, −*y*, −*z*.

Table 4. Chemical proportions on the Hirshfeld surface around the organic moiety, the Cu(II) cation and the two acetate anions. Hc and Hn represent the hydrogen atoms bound to carbon and nitrogen, respectively. Actual contact types and their enrichment in the crystal packing of the title compound are then given. The major contacts and the most enriched are highlighted in bold.

atom	Hn	C	N	O	Cu	Hc
% surf.	6.9	19.7	8.0	17.4	10.3	37.8
Hn	0.2					
C	1.0	5.9		Contacts		(%)
N	2.8	1.3	0.0			
O	2.4	0.8	0.0	0.0		
Cu	1.1	2.7	4.5	**17.5**	1.2	
Hc	6.3	**18.5**	6.3	9.3	3.0	**15.2**
Hn	0.4					
C	0.4	**1.8**			Enrichment	
N	**2.7**	0.5	0.00			
O	1.2	0.16	0.00	0.01		
Cu	0.5	0.5	**1.9**	**3.5**	0.5	
Hc	1.2	**1.4**	1.1	0.8	0.26	1.1

Table 5. Mulliken charge transfer in the title complex.

Atom	**Charge**	
Cu	-0.217248	
Acetate		
C(O)	1.115979	1.186813
O	-0.274461 -0.428773	-0.231182 -0.293471
C(H)	-1.317243	-1.477594
H	0.236834 0.231583 0.231618	0.227513 0.228611 0.231228
Organic molecule		
N1	-0.206884	
N2	-0.276158	
N3	-0.911644	
H(N3)	0.422814 0.521420	
C1	0.570691	
C2	-0.065855	
H(C2)	0.228217	
C3	-0.030284	
H(C3)	0.185603	
C4	0.273518	
C5	-0.827291	
H(C5)	0.232086 0.203364 0.230023	

Supplement

Sup X-ray single crystal structural analysis

The crystal-to-detector distance was 40 mm and the exposure time was 10 seconds per frame for all sets. The scan width was 0.5°. Data collection was 99.8% complete to 25° in θ. A total of 20708 reflections were collected covering the indices, $-9 \le h \le 9$, $-11 \le k \le 11$, $-13 \le l \le 13$. 2848 reflections were symmetry independent and the $R_{int} = 0.0197$ indicated that the data was brilliant. Indexing and unit cell refinement indicated a triclinic lattice. The space group was found to be P $\bar{1}$ (No. 2). The data were integrated and scaled using SAINT, SADABS within the APEX2 software package by Bruker [S1]. Solution by direct methods (SHELXS, SIR97) [S2] produced a complete heavy atom phasing model consistent with the proposed structure. The structure was completed by difference Fourier synthesis with SHELXL97 [S3, S4]. Scattering factors are from Waasmair and Kirfel [S5]. Hydrogen atoms were placed in geometrically idealized positions and constrained to ride on their parent atoms with C-H distances in the range 0.95-1.00 Å. Isotropic thermal parameters U_{iso} were fixed such that they were $1.2U_{eq}$ of their parent atom for CH's and $1.5U_{eq}$ of their parent atom in case of methyl groups.

References

[S1] A.R. Katritzky, C.W. Pees, A.J. Boulton, C. Mckillop, J. Heterocycl. Chem. **3**, 57 (1984).

[S2] T.W. Lane, F.M. Morel, Proc. Natl. Acad. Sci. U. S. A. **97**, 4627 (2000).

[S3] R. Karmakar, C.R. Choudhury, D.L. Hughes, S. Mitra, Inorg. Chim. Acta **360**, 2631 (2007).

[S4] J.-C. Dai, X.-T. Wu, Z.-Y. Fu, C.-P. Cui, S.-M. Hu, W.-X. Du, L.-M. Wu, H.-H. Zhang, Inorg. Chem. **41**, 1391 (2002).

[S4] Y.-H. Liu, Y.-L. Lu, H.-C. Wu, J.-C. Wang, K.-L. Lu, Inorg. Chem. **41**, 2592 (2002).

Sup Chemical preparation

Anal. Calc.: C, 37.14; H, 4.47; N, 14.44 %. Found: C, 37.53; H, 4.22; N, 14.37 %.

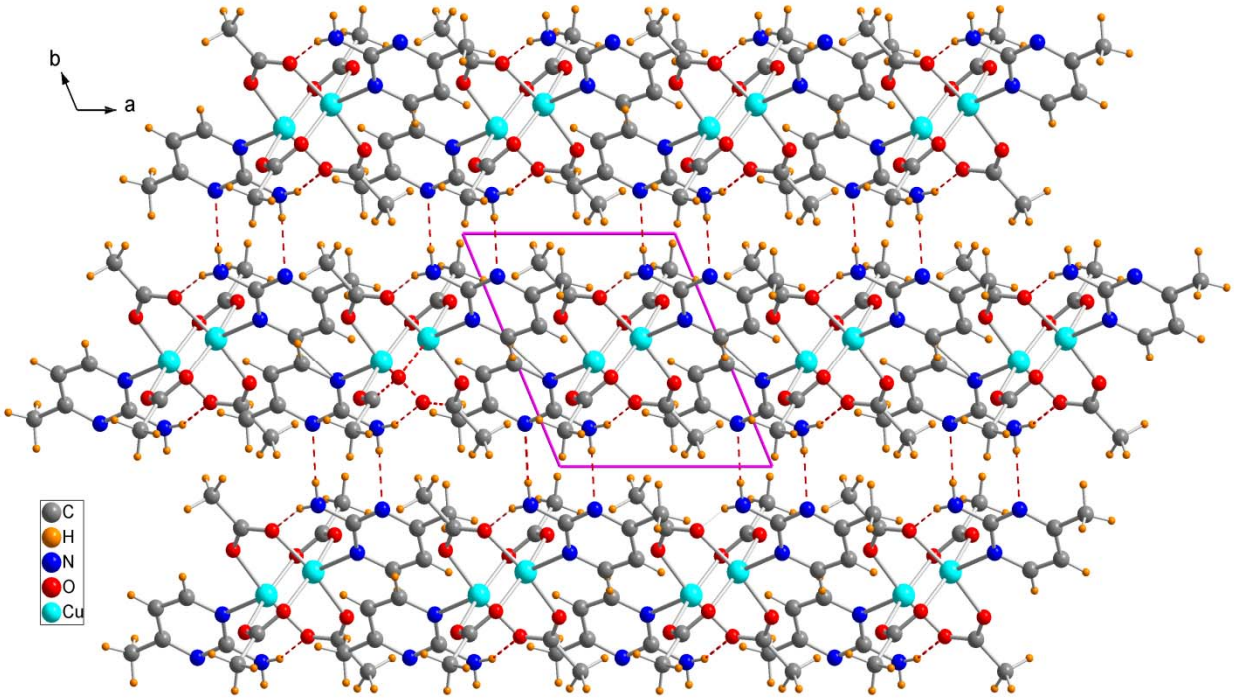

Fig. S1. Crystal packing arrangement of $[Cu_2(CH_3COO)_4(C_5N_3H_7)_2]$ viewed along *c*-axis. Dotted lines indicate hydrogen bonds.